SIMB
Society for Industrial Microbiology and Biotechnology

METABOLIC ENGINEERING AND SYNTHETIC BIOLOGY - ORIGINAL PAPER

CrossMark

Rational design of a synthetic Entner–Doudoroff pathway for enhancing glucose transformation to isobutanol in *Escherichia coli*

Shaoxiong Liang[1,2] · Hong Chen[1,2] · Jiao Liu[1,2] · Jianping Wen[1,2]

Abstract

Isobutanol as a more desirable biofuel has attracted much attention. In our previous work, an isobutanol-producing strain *Escherichia coli* LA09 had been obtained by rational redox status improvement under guidance of the genome-scale metabolic model. However, the low transformation from sugar to isobutanol is a limiting factor for isobutanol production by *E. coli* LA09. In this study, the intracellular metabolic profiles of the isobutanol-producing *E. coli* LA09 with different initial glucose concentrations were investigated and the metabolic reaction of fructose 6-phosphate to 1, 6-diphosphate fructose in glycolytic pathway was identified as the rate-limiting step of glucose transformation. Thus, redesigned carbon catabolism was implemented by altering flux of sugar metabolism. Here, the heterologous Entner–Doudoroff (ED) pathway from *Zymomonas mobilis* was constructed, and the adaptation of upper and lower parts of ED pathway was further improved with artificial promoters to alleviate the accumulation of toxic intermediate metabolite 2-keto-3-deoxy-6-phospho-gluconate (KDPG). Finally, the best isobutanol-producing *E. coli* ED02 with higher glucose transformation and isobutanol production was obtained. In the fermentation of strain *E. coli* ED02 with 45 g/L initial glucose, the isobutanol titer, yield and average producing rate were, respectively, increased by 56.8, 47.4 and 88.1% to 13.67 g/L, 0.50 C-mol/C-mol and 0.456 g/(L × h) in a shorter time of 30 h, compared with that of the starting strain *E. coli* LA09.

Keywords *Escherichia coli* · Isobutanol · Glucose transformation · Metabolic profiles · Heterologous ED pathway

Introduction

As an important platform chemical compound, isobutanol has been widely applied in several fields, including food, pharmaceutical, chemical and so on [19]. It has been also considered as a more desirable biofuel with advantages of higher energy density and vapor pressure, lower hygroscopicity and corrosivity [42]. Compared with the bio-ethanol, bio-isobutanol has a higher renewable identification number; therefore, it is possible to replace bio-ethanol as an ideal gasoline additive or substitute [21]. However, high isobutanol-producing strains have not been existed in nature, while valine metabolism pathway in *Saccharomyces cerevisiae* was generally exploited to construct artificial isobutanol synthesis pathway (*Ehrlich* pathway) in host microbes such as *Escherichia coli* [8], *Bacillus subtilis* [12], *Saccharomyces cerevisiae* [5] and *Corynebacterium glutamicum* [40]. Recently, the biosynthesis of isobutanol has received much attention; yet most of those have centered on more economical biosynthesis by engineering various strains with higher isobutanol production or cheaper feedstock utilization [2, 4, 24, 29, 40].

To improve production of isobutanol, many efforts have been done to identify the limiting factors of isobutanol biosynthesis. By elementary flux mode analysis, Li et al. [23, 34] predicted that pentose phosphate pathway and transhydrogenase were important targets for isobutanol synthesis by regulating the intracellular NADPH production in *Bacillus subtilis*, as isobutanol synthesis is NADPH dependent.

✉ Jianping Wen
jpwen@tju.edu.cn

1 Key Laboratory of Systems Bioengineering (Ministry of Education), Tianjin University, Tianjin 300072, People's Republic of China

2 SynBio Research Platform, Collaborative Innovation Center of Chemical Science and Engineering (Tianjin), School of Chemical Engineering and Technology, Tianjin University, Tianjin 300072, People's Republic of China

Using a genome-scale metabolic model (GSMM), the GAPD reaction catalyzed via the glyceraldehyde-3-phosphate dehydrogenase was predicted as the key target for redox status improvement in *E. coli*. And then, an isobutanol-producing *E. coli* LA09 [27] was achieved by rationally designing, engineering, and fine-tuning the expression of *gapN* gene. Nevertheless, the glucose transformation to isobutanol was low in the fermentation characteristics of *E. coli* LA09.

To achieve a greater carbon utilization efficiency, most researchers tend to extend the carbon source spectrum [11, 28] or increase carbon uptake rate based on metabolic engineering [11]. The glycolytic pathway is the center of the carbon metabolism, which provides energy, cell component precursors and fermentation products in the life span; so, it is an underlying engineering target for improving the bioconversion efficiency [16]. The feedback inhibition and transcriptional repression of key enzymes would often be resolved by screening resistance bacteria and gene over-expression, but glycolytic pathway is an important target generally recognized difficult for manipulation [15, 41]. Since the glucose metabolism is under the control of multi-enzymatic reactions including transcriptional regulation, protein activity regulation and allosteric control of end metabolites [32], glycolytic pathway exhibits very strong robustness, and simple genetic modification is difficult to break constraint of natural evolution [13, 15, 16, 36, 41].

In addition to glycolytic pathway, there are three major kinds of carbohydrate metabolism pathways in nature, i.e., pentose-phosphate (PP), Entner–Doudoroff (ED) and phosphoketolase (PK). (1) Among them, ED pathway has the least reaction steps, requires several-fold less enzymatic protein than the glycolytic pathway to sustain the same flux [9, 30], implying that ED pathway is a lower consuming pathway. (2) One molecular NADPH is generated from one molecular glucose 6-phosphate by PP, PK and ED pathway, respectively, which hold the same advantage from the point of redox. (3) There is one carbon loss per glucose by PP and PK pathway, respectively, but no carbon loss by ED pathway. Based on the above reasons, ED pathway may be the preferential complementary pathway for glucose transformation to isobutanol. ED pathway is encoded by 4 genes, whose upper part is composed of genes *pgl* and *zwf* encoding 6-phosphogluconolactonase and glucose-6-phosphate 1-dehydrogenase, respectively, while the lower part contains the genes *eda* and *edd* encoding 2-dehydro-3-deoxyphosphogluconate aldolase and 6-phosphogluconate dehydratase. *E. coli* contains genes encoding a few enzymes of the ED pathway, but the research showed that ED pathway in *E. coli* was not an efficient metabolism pathway, because it was severely hampered by transcription, translation and allosteric regulation [35]. However, the ED pathway widely exists in most *Pseudomonas* and *Zymomonas* [9]. Especially for *Zymomonas mobilis*, ED pathway completely dominates the

glucose metabolism. It had been reported that ED pathway of *Zymomonas mobilis* is very efficient in nature, attributed to the higher expression, higher conversion efficiency and lower allosteric regulation of ED pathway enzymes [7, 17, 30]. Therefore, it is a better choice to construct an artificial ED pathway in *E. coli* to promote the glucose transformation for isobutanol production based on the ED pathway of *Zymomonas mobilis*.

In this study, the isobutanol-producing *E. coli* LA09 [27] constructed by our group was used in the fermentation research with various initial glucose concentrations. Based on gas chromatograph–mass spectrometer (GC–MS), liquid chromatography–mass spectrometry/mass spectrometry (LC–MS/MS) and high-performance liquid chromatography (HPLC) datasets, the intracellular metabolism of *E. coli* LA09 was investigated to identify the key metabolites significantly associated with isobutanol production and rate-limiting steps of glucose transformation. Then, the artificial heterologous ED pathway was redesigned and engineered, furthermore modulated by artificial promoters to obtain a high-efficient *E. coli* strain for isobutanol production. Finally, the fermentation characteristics of the best strain were investigated.

Materials and methods

Bacterial strains and plasmids

The previously reported isobutanol-producing *E. coli* LA09 (derivative of *E. coli* MG1655) [27] was used as the starting strain. Strains *E. coli* EDA and *E. coli* ED01–ED06 were engineered in this study, respectively. The strains and plasmids used in this study are listed in the supplementary material (Supplementary Materials: Table S3), and all the primers used in this study could be found in supplementary material (Supplementary Materials: Table S4). DNA manipulation techniques for strains and plasmids construction were carried out by standard protocols [6]. Unless otherwise noted, all enzymes were purchased from Fermentas Co., Ltd (Glen Burnie, MD, USA). Oligonucleotides were synthesized by Invitrogen Biotechnology Co., Ltd (Carlsbad, CA, USA), and DNA sequencing was served by BGI (Beijing, China).

Medium and culture conditions

M9 medium was used for isobutanol fermentation supplemented with the required glucose, 5 g/L yeast extract, and 1000th dilution of Trace mix A5. Ampicillin and chloramphenicol (Sangon Biotech, Shanghai, China) were added appropriately. M9 media contained 17 g/L $Na_2HPO_4 \cdot 12H_2O$, 3 g/L KH_2PO_4, 0.5 g/L NaCl, 1 g/L NH_4Cl, 0.24 g/L $MgSO_4$, and 0.011 g/L $CaCl_2$. Trace mix A5 was

composited of 2.86 g/L H_3BO_3, 1.81 g/L $MnCl_2 \cdot 4H_2O$, 0.222 g/L $ZnSO_4 \cdot 7H_2O$, 0.39 g/L $NaMoO_4 \cdot 2H_2O$, 0.079 g/L $CuSO_4 \cdot 5H_2O$, and 49.4 mg/L $Co(NO_3)_2 \cdot 6H_2O$ [1].

Pre-cultures of isobutanol fermentation were conducted in test tubes containing 3 mL of the supplemented M9 medium for 12 h at 37 °C. Fermentations were inoculated with 1% pre-cultures in 250 mL flasks containing 20 mL the supplemented M9 medium. After 4-h cultivation at 37 °C and 200 rpm, the OD_{600} value of cell culture reached to 0.7; subsequently, 0.1 mM isopropyl-β-D-thiogalactoside (Sigma-Aldrich, St. Louis, MO, USA) was added to the medium. The flasks were sealed tightly with rubber stoppers. And then cultivation was further performed at 30 °C and 200 rpm.

GC–MS and LC–MS/MS analysis

To analyze the intracellular metabolic response of *E. coli* LA09 on different initial glucose concentrations (35, 40, 45, 50, 55 and 60 g/L), GC–MS and LC–MS/MS were performed for intracellular metabolites analysis. The cells collected at exponential phase (20 h) would be immediately quenched by 60% methanol (− 40 °C, v/v) after taking from the fermentation broth. Then, the extraction, determination and analysis of intracellular metabolites were performed according to the previous described methods [43, 44]. Succinic d_4 (St. Louis, MO, USA) and D-sorbitol-$^{13}C_6$ (St. Louis, MO, USA) would be added in advance and served as the internal standard for GC–MS analysis and LC–MS/MS analysis, respectively. LC–MS/MS measurements of metabolites only included sugar phosphate intermediates of pentose-phosphate pathway and glycolytic pathway, such as glucose 6-phosphate, fructose 6-phosphate, fructose 1,6-biosphosphate, glyceraldehyde 3-phosphate, phosphoenolpyruvate, erythrose 4-phosphate, ribose 5-phosphate, ribulose 5-phosphate, xylulose 5-phosphate and sedoheptulose 7-phosphate. All the chemicals used in the metabolome isolation, GC–MS and LC–MS/MS analysis were purchased from Sigma-Aldrich (St. Louis, MO, USA).

Determination of NAD(P) and NAD(P)H concentrations

The intracellular NAD(P) and NAD(P)H were determined by high-performance liquid chromatography (HPLC) following extraction as in previous descriptions [10, 25, 27]. Cells were harvested by centrifugation (4 °C, 1 min, 10,000 rpm) at exponential phase (20 h); the pellet was resuspended in 1.0 mL of 0.3 M HCl to extract the oxidized forms or 1.0 mL of 0.3 M KOH to extract the reduced forms. After heating at 50 °C for 10 min, all samples were cooled on ice to 0 °C. And then, neutralization was performed by adding 0.3 mL of 0.1 M KOH for oxidized forms or 0.3 mL of 0.1 M HCl for

reduced forms. The cellular debris was removed by centrifuging (4 °C, 5 min, 15,000 rpm). Supernatants were transferred to new tubes. Then, the NAD(P) and NAD(P)H were determined by a HPLC system using Synergi™ Hydro-RP column (250 mm × 4.6 mm, 4 μm, Phenomenex, USA) as column with operating temperature at 30 °C. The mobile phase consisted of 80% A and 20% B (A: 0.2 M phosphate buffer containing 10 mM tetrabutyl ammonium bromide, pH 7.0; B: methanol). The flow rate was 0.8 mL/min and the detection wavelength was 254 nm. The standards of cofactors were purchased from Sigma-Aldrich (St. Louis, MO, USA).

Data processing and multivariate statistical analysis

The data analysis was performed as previous described [43, 44]. The peak area of each metabolite was normalized to the internal standard succinic acid d_4 and cell biomass in GC–MS analysis. Absolute metabolite concentrations determined by LC–MS/MS in extracts were normalized to the biomass and internal standard D-sorbitol-$^{13}C_6$. Concentrations of NAD(P) and NAD(P)H measured by HPLC were normalized to the biomass. Both of the normalized metabolites between GC–MS and LC–MS/MS analysis, as well as NAD(P) and NAD(P)H were combined together finally. The relative abundance matrix of the whole identified metabolites at each sampling point was imported into SIMCA-P package (Ver 11.5; Umetrics, Umea, Sweden) for the multivariate statistical analysis. In this study, five biological replicates were used to perform multivariate analysis for each sample condition, and the experimental data were calculated as the mean value with the error indicated by the standard deviation.

Construction of strain *E. coli* EDA and ED01 with initial synthetic ED pathway

The integration fragments of upper and lower part of the ED pathway were constructed using overlap PCR method [14], and then integrated into the chromosome of host strain *E. coli* LA01 to obtain strain *E. coli* EDA and ED01, detail steps are as follows:

(1) The lower part construction of the ED pathway: the genes ZMO0368 and ZMO0997 under the control of BBa_J23119 promoter were amplified from *Z. mobilis* ZM4 with primer sets z368-F1/z368-R and z997-F/z997-R, respectively. Gentamicin-resistant fragment was amplified from pUCxer plasmid with primer set XER2-F/XER2-R. Then, the three fragments were combined using overlap PCR method to generate the operon fragment ZMO0368-ZMO0997-dif-Xer-dif which was verified by gene sequencing.

Next, the integration fragment of lower part of the ED pathway was obtained by amplifying the operon fragment ZMO0368-ZMO0997-dif-Xer-dif with primer set ack-pta-F/ack-pta-R containing the homologous arms of the gene *ack-pta* in *E. coli* LA01. Then, the lower part integration fragment of the ED pathway was integrated into the chromosome of host strain *E. coli* LA01; the positive recombination strain *E. coli* LA01 Δ*ackA-pta*::(BBa_J23119::ZMO0368-ZMO0997-dif-Xer-dif) was selected using gentamicin screening, and then verified by Colony PCR with primer set Test2-F/Test2-R. Finally, *E. coli* LA01 Δ*ackA-pta*::(BBa_J23119::ZMO0368-ZMO0997) was obtained by incubated at 42 °C to remove the gentamicin resistant cassette.

(2) The upper part construction of the ED pathway: the genes ZMO0367 and ZMO1487 under the control of BBa_J23119 promoter were amplified from *Z. mobilis* ZM4 with primer sets z367-F1/z367-R and z1487-F/z1487-R, respectively. Gentamicin-resistant fragment was amplified from pUCxer plasmid with primer set XER1-F/XER1-R. Then the three fragments were combined using overlap PCR method to generate the operon fragment ZMO0367-ZMO1487-dif-Xer-dif which was verified by gene sequencing. Next, the integration fragment of upper part of the ED pathway was obtained by amplifying the operon fragment ZMO0367-ZMO1487-dif-Xer-dif with primer set ldh-F/ldh-R containing the homologous arms of the gene *ldhA* in *E. coli* LA01. Then, the upper part integration fragment of the ED pathway was integrated into the chromosome of *E. coli* LA01 Δ*ackA-pta*::(BBa_J23119::ZMO0368-ZMO0997); the positive recombination strain *E. coli* LA01 Δ*ackA-pta*::(BBa_J23119::ZMO0368-ZMO0997) Δ*ldhA*::(BBa_J23119::ZMO0367-ZMO1487-dif-Xer-dif) was selected using gentamicin screening, and then confirmed by Colony PCR with primer set Test1-F/Test1-R. Then, after incubation at 42 °C to remove the gentamicin-resistant cassette, strain *E. coli* LA01 Δ*ackA-pta*::(BBa_J23119::ZMO0368-ZMO0997) Δ*ldhA*::(BBa_J23119::ZMO0367-ZMO1487) was obtained.

(3) Finally, pACYCLA09 and pTRCLA17 were both transformed into *E. coli* LA01 Δ*ackA-pta*::(BBa_J23119::ZMO0368-ZMO0997) generating the strain *E. coli* EDA containing the lower part of ED pathway. And pACYCLA09 and pTRCLA17 were both transformed into *E. coli* LA01 Δ*ackA-pta*::(BBa_J23119::ZMO0368-ZMO0997) Δ*ldhA*::(BBa_J23119::ZMO0367-ZMO1487) generating the strain *E. coli* ED01containing the whole ED pathway.

Construction of strain *E. coli* ED02–ED06 with modulating the ED pathway

The gene expressing modulation of the upper and lower parts of the ED pathway were performed using constitutive promoters, the details was as following: (1) the constitutive promoters BBa_J23105, BBa_J23118 and BBa_J23119 was from the Registry of Standard Biological Parts (http://partsregistry.org/). (2) These constitutive promoters were synthesized in the primers z367-F1, z367-F2, z367-F3, z368-F1 and z368-F2, respectively. Promoter z367-F1 containing BBa_J23119, z367-F2 containing BBa_J23118 and z367-F3 containing BBa_J23105 were used for modulating the upper part of ED pathway, while z368-F1 containing BBa_J23119 and z368-F2 containing BBa_J23118 were used for modulating the lower part of ED pathway. (3) The strains ED02–ED06 were constructed with the same method of the strain ED01. The detail primers used for the strains ED01–ED06 were shown in supplementary material (Supplementary Materials: Table S2).

mRNA levels of ZMO0367 and ZMO0368 detected by RT-PCR

The mRNA levels of ZMO0367 and ZMO0368 were determined by RT-PCR, according to Lin et al. [26]. The recombinant strains were cultured with 45 g/L glucose. Cells were harvested at OD_{600} of 4.0. Total mRNA were extracted using the CellAmp® Direct RNA Prep Kit (Takara, Dalian, China) as described by the manufacturer. The cDNA was amplified using Prime Script™ RT reagent Kit (Takara, Dalian, China) with the total mRNA as the templates. Samples were then analyzed using Bio-Rad iQ5 Real Time PCR (Bio-Rad, USA) with SYBR® Premix Ex Taq™ (Takara, Dalian, China). RT-PCR amplification primers were given in supplementary material (Supplementary Materials: Table S4). The 16S rRNA gene was selected as internal standard. The obtained data were analyzed by using the $2^{-\Delta\Delta Ct}$ method described by Schmittgen and Livak [37].

Analytical methods

Cell growth was monitored by optical density measurements at 600 nm and converted to DCW concentration using the value of 0.332 g/L DCW per unit OD determined. Glucose concentration was measured with a biosensor analyser (SBA-40C, Shandong, China). Isobutanol was quantified by a gas chromatograph (430-GC, Brucker, USA) with a flame ionization detector as described by Liu et al. [27]. A BW-SWAX capillary column (Brucker, USA) was used. GC oven temperature was initially held at 80 °C for 2 min, then raised to 120 °C with a gradient 10 °C/min and held for 2 min. And followed by raising with a gradient 50 °C/

min until 230 °C and held for 2 min. Nitrogen was used as the carrier gas at 1.0 mL/min. 1 μL aliquot was injected with 1-butanol as internal standard. To quantify acetic acid and lactic acid, sample (10 μL) was injected into HPLC (1200, Agilent Technologies, USA) equipped with Synergi™ Hydro-RP column (250 mm × 4.6 mm, 4 μm, Phenomenex, USA) as described by Liu et al. [27]. The mobile phase was 5 mM H_2SO_4 at a flow rate of 0.8 mL/min with detection wavelength of 210 nm. The column was operated at 30 °C. Unless otherwise noted, high-purity chemical standards were all purchased from Sangon Biotech (Shanghai, China).

Statistical analysis

Five biological replicates were used to perform metabolic profiling for each sample. Five independent biological replicates were performed in fermentations for every sample, and the experimental data were calculated as the mean value with the error indicated by the standard deviation. All figures were made by SigmaPlot software.

Results

Identification limiting factors of glucose transformation by intracellular metabolic profiling

A series batch fermentation of the starting strain *E. coli* LA09 had been performed under the different initial glucose concentrations (35, 40, 45, 50, 55 and 60 g/L glucose). As shown in Fig. 1, at the end of isobutanol fermentation, the isobutanol titer had been increased from 8.62 to 8.91 g/L when the initial glucose concentration varied from 35 to 45 g/L. But the opposite trend could be observed along with the initial glucose concentration continued to increase to 60 g/L (Fig. 1b). Interestingly, the similar trend had also been found in the biomass (Fig. 1a), which reached a peak of 2.42 g/L with the initial glucose concentration of 45 g/L. It indicated that the increase of initial glucose concentration (from 35 to 45 g/L) was benefited for isobutanol and biomass accumulation. But the synthesis of biomass and isobutanol would be obviously inhibited in the high glucose concentration (45–60 g/L). Specifically, the specific glucose uptake rate was continuously increased from 0.760 to 0.885 g/g/h as the initial glucose concentration shifted from 35 to 60 g/L, while the increase trend became slower when the initial glucose concentration was over 45 g/L (Fig. 1c), which was almost consistent with the previous report [22]. Conversely, the


Fig. 1 The fermentation characteristics of isobutanol-producing strain *E. coli* LA09 with different initial glucose concentrations (35 to 60 g/L). **a** Biomass, **b** isobutanol, **c** specific glucose uptake rate, d isobutanol yield. The values shown represent the means of five independent experiments and the error bars represent standard deviations of five values
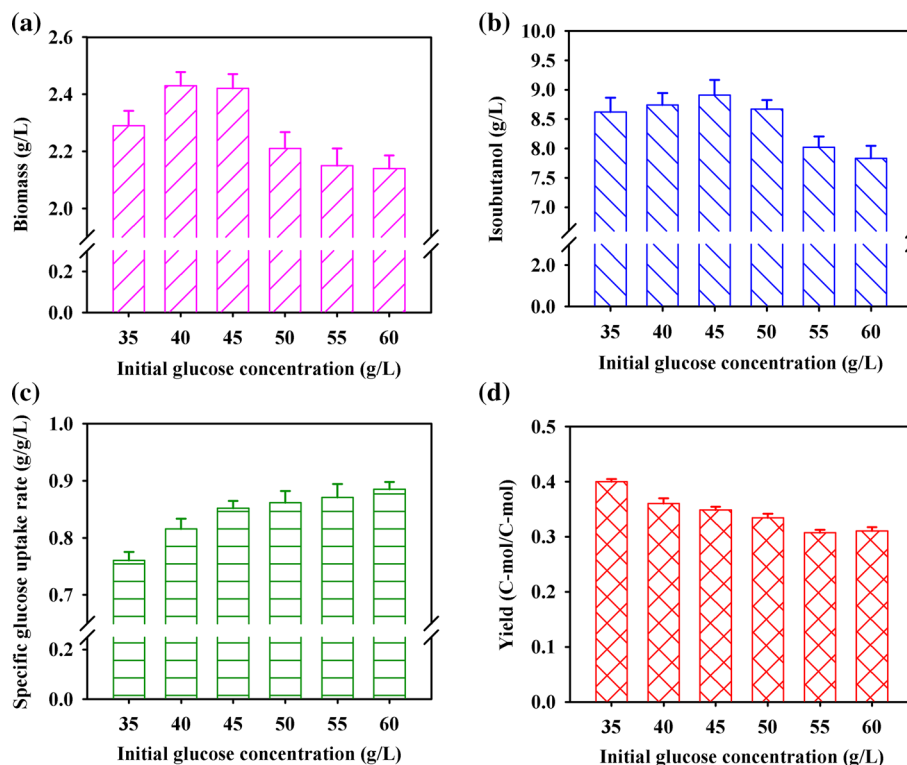
isobutanol yield was decreased from 0.40 to 0.31 C-mol/C-mol (Fig. 1d). The increase of initial glucose concentration promoted the glucose uptake, but it emerged a reverse trend of isobutanol yield. So, it was speculated that the limiting factors was not in the uptake of glucose but in the intracellular carbon catabolism. In addition, acetic acid and lactic acid were also detected by HPLC. The concentration of acetic acid increased from 0.5 to 0.8 g/L with the increase of initial glucose concentration from 35 to 50 g/L, but reduced to 0.6 g/L when the initial glucose concentration increased to 60 g/L. At the same time, the concentration of lactic acid increased from 6.08 to 7.15 g/L with a rise of initial glucose concentration from 35 to 50 g/L, and was almost unchanged with the further increase of initial glucose concentration (50–60 g/L). The accumulation of acetic acid and lactic acid were increased very little; thus, there were no significant changes of the final pH values of fermentation broth (from 5.6 to 5.4). Therefore,

the accumulation of organic acids (such as acetic acid and lactic acid) might have lower effects on the synthesis of biomass and isobutanol.

Metabolites profiles and multiple statistical analyses of the above isobutanol fermentations with different initial glucose concentrations (35–60 g/L) had been performed to search the limiting factors of glucose transformation. A total of 93 intracellular metabolites, including 79 metabolites such as amino acids, organic acids, sugars, alcohols, lipids and so on by GC–MS analysis, 10 sugar phosphate by LC–MS/MS analysis and 4 redox cofactors by HPLC analysis, were identified in 30 samples for all conditions. (Supplementary Materials: Table S1). As shown in Fig. 2, all of the 93 metabolites were further analyzed using principal component analysis (PCA) and partial least square-discriminant analysis (PLS-DA). PCA analysis (Fig. 2a) revealed the following features: (1) all of the same treated samples (five parallels) could be obviously clustered together,
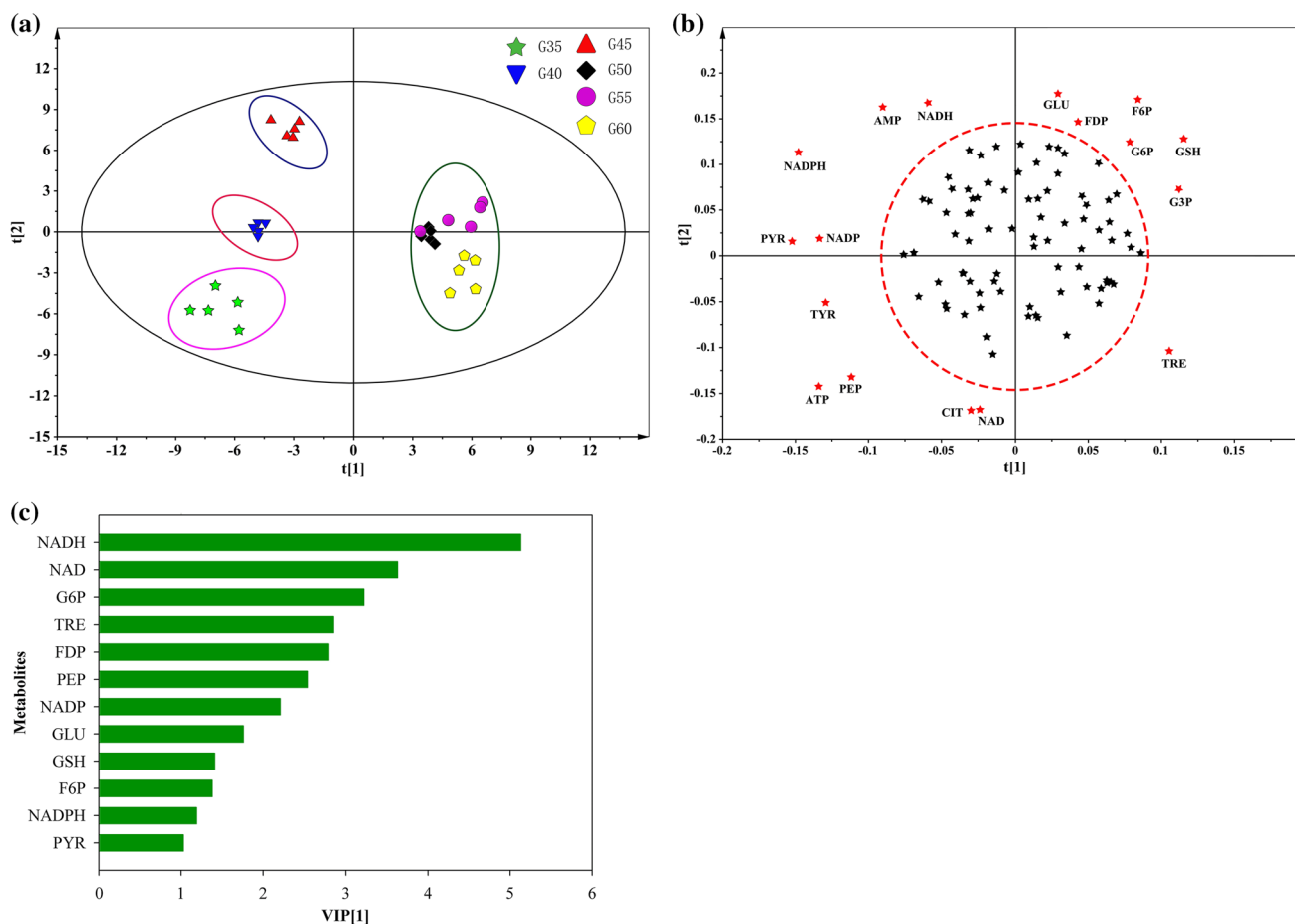
Fig. 2 PCA and PLS-DA analysis of GC–MS, LC–MS/MS and HPLC metabolites profiles. **a** PCA-derived score plots. G35 represents the initial glucose concentration of 35 g/L, and so on. **b** PCA-derived loading plots. **c** PLS-DA-derived loading plots. *T1* and *T2* are referred as the scores of projection 1 and 2 in PCA analysis, respectively. *PYR* pyruvate, *F6P* fructose 6-phosphate, *GSH* glutathione, *GLU* L-Glutamate, *PEP* phosphoenolpyruvate, *FDP* fructose 1,6-bisphosphate, *TRE* trehalose, *G6P* glucose-6-phosphate, *G3P* glyceraldehyde 3-phosphate, *TYR* tyrosine, *CIT* citrate

respectively; (2) the differently treated samples could be separated completely with each other except G50, G55 and G60 (corresponding to initial glucose concentration of 50, 55 and 60 g/L), indicating the different intracellular metabolic characteristics with low initial glucose concentration (35, 40 and 45 g/L), but similar characteristics under high initial glucose concentration (50, 55 and 60 g/L). Moreover, the contribution of each metabolite to a specific component was reflected by loading value, as shown in Fig. 2b. Those metabolites with the higher loading values have more significant influence on the differences. Here, 17 metabolites were observed to be separated clearly from others and were identified to be the most significant metabolites responsible for the discrimination among the conditions of different initial glucose concentrations.

To further identify metabolites closely associated with isobutanol production, we performed PLS-DA (using isobutanol titer as the Y matrix) for all samples with different initial glucose concentrations (35–60 g/L). The variable importance of the projection plots (VIP) score for each mass peak was generated by PLS-DA analysis (Supplementary Materials: Table S1). A higher VIP score implied that the peak contributed more significantly towards the differentiation of high and low isobutanol production. A total of 12 metabolites (VIP score > 1) were identified and selected for further investigation (Fig. 2c). Among the above identified 12 metabolites, it was obvious that glycolytic pathway (EMP) pathway (glucose 6-phosphate, fructose 6-phosphate, fructose 1, 6-bisphosphate, phosphoenolpyruvate and pyruvate), cofactor metabolism (NAD, NADH, NADP, NADPH) and stress response compounds (trehalose, ʟ-glutamate and glutathione) might be the key metabolic pathways in different initial glucose concentration. According to the previous report [27], NADPH availability has a strong correlation with isobutanol production. Here, the PLS-DA analysis (Fig. 2c) showed that NADPH had relative lower impact on isobutanol production. The main reason might be the redox status improvement by the construction of heterogenous gapN-encoding NADP dependent glyceraldehyde-3-phosphate dehydrogenase pathway [27]. Hence, NADPH was no more a limiting factor for isobutanol production in *E. coli* LA09 and had relative lower impact on isobutanol production in PLS-DA analysis. However, PLS-DA analysis of metabolomic data showed that lactic acid and acetic acid had no strong correlations with isobutanol biosynthesis. Notably, the glycolytic pathway was the main pathway of the glucose transformation to isobutanol [1]. Thus, the metabolites in glycolytic pathway would be further analyzed in detail.

As shown in Fig. 3, as the initial glucose concentration increased from 35 to 45 g/L, the relative abundance of glucose 6-phosphate (G6P), fructose 6-phosphate (F6P), fructose 1, 6-bisphosphate (FDP), glyceraldehyde 3-phosphate (G3P), glycerate 3-phosphate (3PG), glycerate 2-phosphate

(2PG), phosphoenolpyruvate (PEP) and pyruvate (PYR) in glycolytic pathway were elevated by 2.68, 1.91, 1.36, 1.16, 1.16, 1.19, 0.31 and 1.27-fold, respectively. According to the above results, the increase level of upstream metabolites (G6P and F6P) was 1.91–2.68-fold, much higher than that (1.16–1.36-fold) of downstream metabolites (FDP, G3P, 3PG and 2PG). It meant that the upstream metabolites (G6P and F6P) were largely accumulated compared with the downstream metabolites (FDP, G3P, 3PG and 2PG) as long as the initial glucose concentration increased continuously. Notably, PYR and PEP showed different trends to other downstream metabolites, as they participated in PTS for glucose uptake. G6P and F6P could connect with PP pathway, but our data showed that the metabolites of PP pathway had no significant difference among the all samples based on the PLS-DA analysis (Fig. 2b). Likewise, the similar result could be observed for the downstream metabolites. So, the reaction from F6P to FDP might be a rate-limiting step to result in the different increase between its upstream and downstream metabolites.

Construction of isobutanol-producing strain with artificial ED pathway for glucose transformation

To relieve the limit from F6P to FDP, the synthetic biological design of heterologous artificial glucose transformation pathway should take into consideration the following three points: (1) the number of steps in the designed pathway; (2) the yields of NADPH and ATP by the designed pathway and (3) the carbon loss from glucose to PYR through the designed pathway.

According to the KEGG database and previous reports [9], four kinds of common glucose catabolic pathways were collected and reconstructed (Supplementary Materials: Fig. S1), containing glycolytic pathway (EMP), pentose-phosphate (PP), phosphoketolase (PK) and Entner–Doudoroff (ED) pathway. The step number, the NADPH yield and the carbon loss of the four pathways were analyzed from its reaction equation in KEGG database (Table 1). The step number of the PP, ED and PK pathway was about half of that of EMP pathway. Among them, ED pathway was only consisting of four steps. According to the analyses of thermodynamics and kinetics, previous report had also been confirmed that ED pathway would only require several-fold less enzymatic protein to achieve the same glucose conversion rate compared with EMP and was substantially more thermodynamically favourable than EMP [9]. Moreover, more NADPH could be yielded through PP, ED and PK pathway, which would facilitate the NADPH-dependent isobutanol synthesis. However, carbon loss was observed both in the PP and PK pathway. And the end metabolites of PP pathway still contained F6P, which meant PP pathway was not a
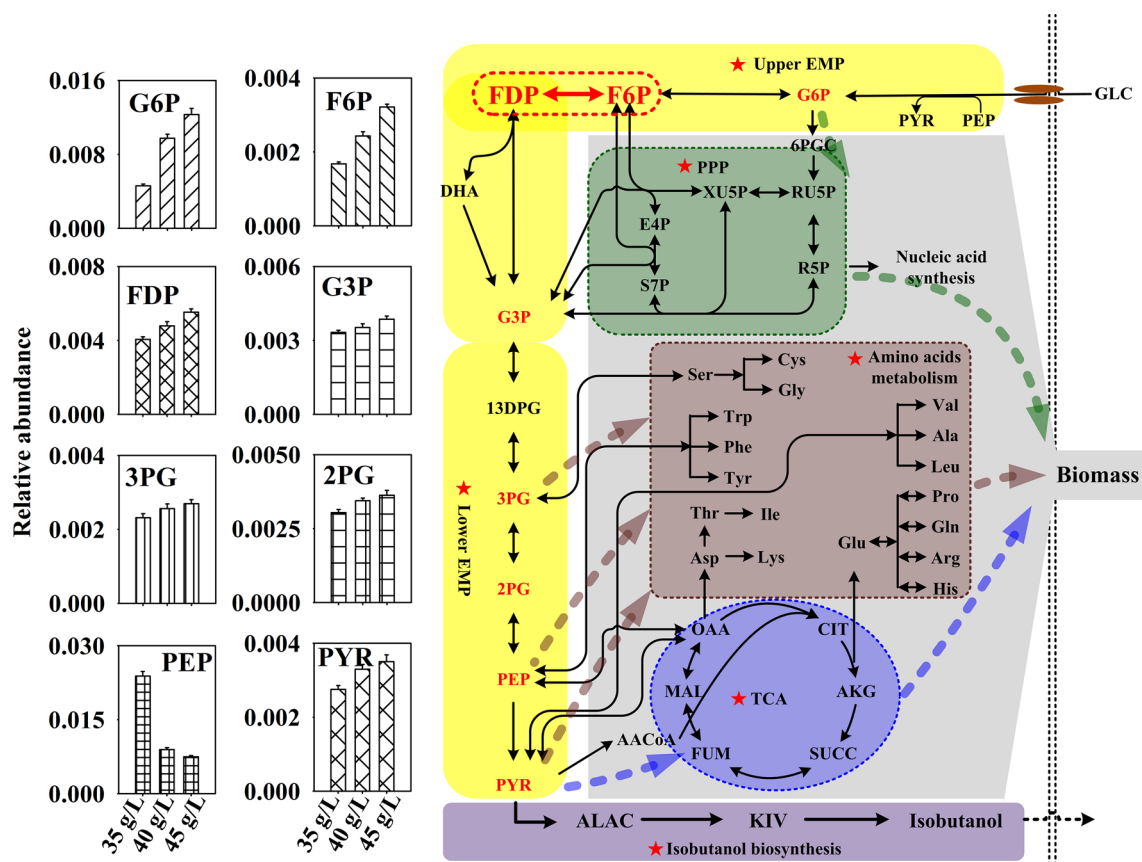
Fig. 3 Changes of intracellular metabolites in EMP pathway. The left part, changes of eight intracellular metabolites in EMP pathway under the conditions of different initial concentrations (35, 40 and 45 g/L). The right part, Schematic diagram of the metabolic pathways closely associated with isobutanol and biomass synthesis. The rate-limiting step is highlighted by red-dotted lines. The key pathways are marked by pentacle. *GlC* glucose, *G6P* glucose-6-phosphate, *F6P* fructose 6-phosphate, *FDP* fructose 1,6-bisphosphate, DHA dihydroxyacetone phosphate, G3P glyceraldehyde 3-phosphate, 13DPG 1,3-diphosphoglycerate, 3PG glycerate 3-phosphate, 2PG glycerate 2-phosphate, PEP phosphoenolpyruvate, PYR pyruvate, 6PGC 6-phospho-gluco-nate, RU5P ribulose 5-phosphate, XU5P xylulose 5-phosphate, R5P ribose 5-phosphate, E4P erythrose 4-phosphate, S7P sedoheptulose 7-phosphate, Ser serine, Cys cysteine, Gly glycine, Trp tryptophan, Phe phenylalanine, Tyr tyrosine, Val valine, Ala alanine, Leu leucine, Thr threonine, Ile isoleucine, Asp aspartate, Lys Lysine, Glu glutamate, Pro proline, Gln glutamine, Arg arginine, His histidine, AACoA acetyl-CoA, OAA oxaloacetate, CIT citrate, AKG 2-oxoglutarate, SUCC succiny-CoA, FUM fumarate, MAL malate, ALAC acetolactate, KIV α-ketoisovalerate. The values shown represent the means of five independent experiments and the error bars represent standard deviations of five values

**Table 1** Characteristics of four glucose catabolism pathways

Pathway	EMP	PP	ED	PK
Step number	9	5	4	5
End products[a]	2 PYR	0.33 F6P 0.33 G3P	1 G3P 1 PYR	1 G3P
ATP[a]	3	0	0	0
NADH[a]	2	0	0	0
NADPH[a]	0	2	2	2
Loss carbon[a]	0	1	0	1

[a]All the numbers of products were calculated from one molecular glucose 6-phosphate

better alternative pathway to overcome the rate-limiting step from F6P to FDP. Based on the above analyses, ED pathway could be considered as the desired pathway to promote the glucose transformation.

The initial ED pathway was constructed using the heterologous genes from the genomic sequenced *Z. mobilis* ZM4 which harbored the most efficient ED pathway in nature [30]. Firstly, the lower part of ED pathway was constructed with the gene ZM4-*edd* (ZMO0368) and ZM4-*eda* (ZMO0997) under the control of the promoter BBa_J23119, and embedded into the host strain to obtain the isobutanol-producing strain *E. coli* EDA. Using the initial glucose concentration of 45 g/L, it could not only find that the fermentation time of *E. coli* EDA had been decreased (Fig. 4a), but also the isobutanol titer was significantly increased from 8.92 to
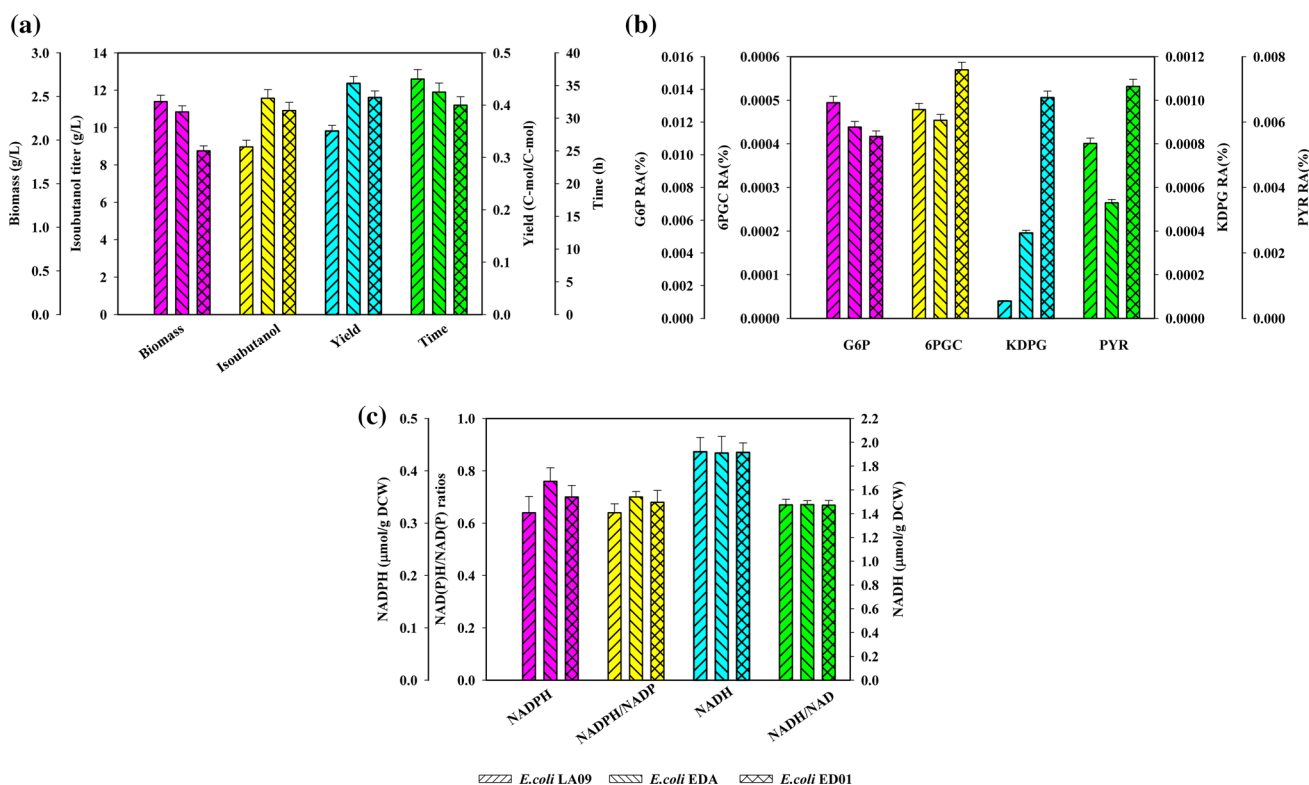
Fig. 4 The fermentation characteristics and pool of intracellular metabolites in ED pathway of *E. coli* LA09, EDA and ED01. **a** Fermentation characteristics, **b** pool of intracellular metabolites in ED pathway, **c** comparison of intracellular redox cofactors at exponential phase. RA represents the relative abundance. The values shown represent the means of five independent experiments and the error bars represent standard deviations of five values

11.52 g/L with the isobutanol yield increased from 0.35 to 0.44 C-mol/C-mol. It could be speculated that the lower part of ED pathway was benefit for the glucose transformation to isobutanol. To further improve the glucose transformation, the upper part of ED pathway was constructed with the gene ZM4-*zwf* (ZMO0367) and ZM4-*pgl* (ZMO1478) under the control of the promoter BBa_J23119, then the isobutanol-producing strain *E. coli* ED01 was obtained with the whole ED pathway.

Compared with the strain *E. coli* EDA, the fermentation time of *E. coli* ED01 could be further decreased (from 34 to 32 h) (Fig. 4a), but the isobutanol titer of *E. coli* ED01 was 10.87 g/L with the yield 0.41 C-mol/C-mol, lower than that of *E. coli* EDA. Meanwhile, the biomass of *E. coli* ED01 was also obviously decreased to 1.85 g/L, lower than that of *E. coli* LA09. The above analysis indicated that the whole ED pathway expression induced the cell growth inhibition which might result in the decrease of glucose transformation and isobutanol production. The main reason may be the inadaptive expression of the ED pathway in host strain.

To further solve the above inadaptive problem, the intracellular metabolites glucose-6-phosphate (G6P), 6-phospho-gluconate (6PGC), 2-keto-3-deoxy-6-phospho-gluconate

(KDPG) and pyruvate (PYR) in the ED pathway were further semi-quantitated and analyzed. Results showed that the intracellular level of G6P could be decreased in both of *E. coli* EDA and *E. coli* ED01 owing to the expression of the gene located in the ED pathway, but the intracellular level of 6PGC, KDPG and PYR could be obviously enhanced, compared with that of *E. coli* LA09 (Fig. 4b). Especially, the intracellular level of the toxic metabolite KDPG in *E. coli* ED01 was dramatically increased by 13.1-fold compared with that of *E. coli* LA09 due to the whole ED pathway expression. And the accumulation of toxic metabolite KDPG was the major factor of cell growth inhibition [30], which ultimately reduced the isobutanol production.

The intracellular redox status was also detected (Fig. 4c). Results showed that the intracellular NADPH concentration and NADPH/NADP ratio (0.38 μmoL/gDCW and 0.70, respectively) of *E. coli* EDA (harboring the lower part of the ED pathway) were higher than that (0.35 ± 0.047 μmoL/gDCW and 0.68, respectively) of *E. coli* ED01 (harboring whole ED pathway), but both of them were higher than that of *E. coli* LA09 (0.32 ± 0.053 μmoL/gDCW and 0.64, respectively), which indicated that the construction of heterologous ED pathway in *E. coli* LA09 would improve the

concentration of NADPH, but it was closely correlated with the efficiency of ED pathway.

## Modulation of ED pathway with different strengthen promoters for further improving glucose conversion

According to the above analysis, the different strength constitutive promoters was used to modulate the upper and lower parts of ED pathway, and other five strains *E. coli* ED02–ED06 were further constructed (Supplementary Materials: Table S3). The $2^{-\Delta\Delta Ct}$ values of the gene expression of ZMO0367 and ZMO0368 in the six strains *E. coli* ED01-ED06 were measured by quantitative real-time reverse transcription PCR (RT-PCR) (Table 2). The $2^{-\Delta\Delta Ct}$ values of ZMO0367 varied from ~ 0.2 to ~ 0.7 and that of ZMO0368 varied from ~ 0.3 to ~ 0.6, indicating the fine-tuned expressions of the upper and lower parts of ED pathway were achieved, which might be helpful for getting an adaptive ED pathway to increase the glucose transformation with high isobutanol production.

From the fermentations profiles of the six strains (Fig. 5a), the clear results could be found as follows: (1) With the upper part of ED pathway under the control of the strongest promoter BBa_J23119 (strains *E. coli* ED01 and *E. coli* ED04), both of cell growth and isobutanol production were suppressed. The biomass of strains *E. coli* ED01 and *E. coli* ED04 was only 1.85 and 1.64 g/L, which were much lower than that of other four strains (2.32 to 2.33 g/L). And the isobutanol titers and yields were relatively low, as well as the fermentation times of *E. coli* ED01 (32 h) and ED04 (34 h) longer than that of other four strains. (2) When the upper part of ED pathway was under the control of the weak promoter BBa_J23105 (strains *E. coli* ED03 and *E. coli* ED06), the modulation of the lower part of ED pathway would not result in obviously change of the transformation of glucose, and the isobutanol titer of *E. coli* ED03 (10.32 g/L) was very similar with that of *E. coli* ED06 (10.25 g/L). (3) When the upper part of ED pathway was under the control of the second stronger promoter BBa_J23118 (strains *E. coli* ED02 and *E. coli* ED05),

Table 2 mRNA levels of ZMO0367 and ZMO0368 in strains *E. coli* ED01–ED06

Strain	ZMO0367	ZMO0368
E. coli ED01	0.71 ± 0.022	0.62 ± 0.020
E. coli ED02	0.43 ± 0.015	0.61 ± 0.023
E. coli ED03	0.23 ± 0.009	0.63 ± 0.023
E. coli ED04	0.72 ± 0.021	0.35 ± 0.010
E. coli ED05	0.44 ± 0.011	0.37 ± 0.012
E. coli ED06	0.21 ± 0.006	0.34 ± 0.011

Gene expression was indicated by the value of $2^{-\Delta\Delta Ct}$
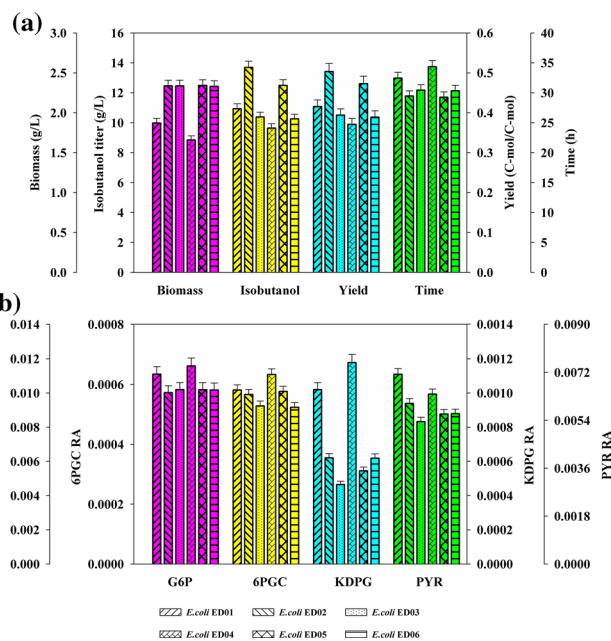
Fig. 5 The fermentation characteristics and pool of intracellular metabolites in ED pathway of *E. coli* ED01-ED06. **a** Fermentation characteristics, **b** pool of intracellular metabolites in ED pathway. RA represents the relative abundance. The values shown represent the means of five independent experiments and the error bars represent standard deviations of five values

the higher expression of the lower part of ED pathway tended to benefit for the glucose transformation to isobutanol. Thus, the strain *E. coli* ED02 with lower part under the control of the strongest promoter BBa_J23119 could produce more isobutanol (13.67 g/L) than *E. coli* ED05 (12.41 g/L) with lower part under the control of the second stronger promoter BBa_J23118. (4) With the upper part of ED pathway under the control of the strongest promoter BBa_J23119, the flux of ED pathway would be limited by the weak expression of the lower part, which could result in the accumulation of G6P and toxic KDPG. The levels of metabolite G6P in *E. coli* ED01 and *E. coli* ED04 were about 12% higher than that in other four strains. Especially, the level of toxic KDPG in *E. coli* ED01 and *E. coli* ED04 were increased by 100% compared with that in other four strains (Fig. 5b).

Overall, the high expression of the upper part of ED pathway would result in the accumulation of toxic KDPG to inhibit cell growth, while the high expression of the lower part of ED pathway would decrease the level of toxic KDPG and be benefit for the glucose transformation.

Comparison of batch fermentation properties of strains *E. coli* ED02 and LA09

The batch fermentation properties of strain *E. coli* ED02 was investigated using the starting strain *E. coli* LA09 as

the control with the initial glucose concentration of 45 g/L (Fig. 6). When the fermentation was finished, the residual glucose of strain ED02 decreased to 0.87 g/L obviously lower than that of LA09 (3.52 g/L). And the fermentation time of ED02 was only 30 h, 16.7% shorter than that of LA09 (36 h). The isobutanol titer of ED02 reached to 13.67 g/L, 56.8% higher than that of LA09, While the biomass of the two strains was very similar (about 2.3 g/L), both of the isobutanol yield and average producing rate were increased by 47.4 and 88.1% to 0.50 C-mol/C-mol and 0.456 g/(L × h) compared with that of the starting strain *E. coli* LA09. This study provided an effective method to rationally design and engineer high-efficient strain for isobutanol production.

Discussion

In our previous work, an isobutanol-producing strain *E. coli* LA02 was constructed by combining NADPH-dependent *Ehrlich* pathway with KIV precursor pathway. Then, the genome-scale metabolic model was applied to investigate the redox cofactor metabolism of the strain *E. coli* LA02. And the GAPD reaction catalyzed by the glyceraldehyde-3-phosphate dehydrogenase was predicted as the key target for redox status improvement. Under guidance of the metabolic model prediction, a heterologous *gapN* was constructed and then fine-tuned. Finally, the strain *E. coli* LA09 was achieved with the isobutanol titer drastically increased [27]. However, the isobutanol production of strain *E. coli* LA09 was still low, and the isobutanol yield was only about half of the maximal theoretical yield of 0.67 C-mol/C-mol.
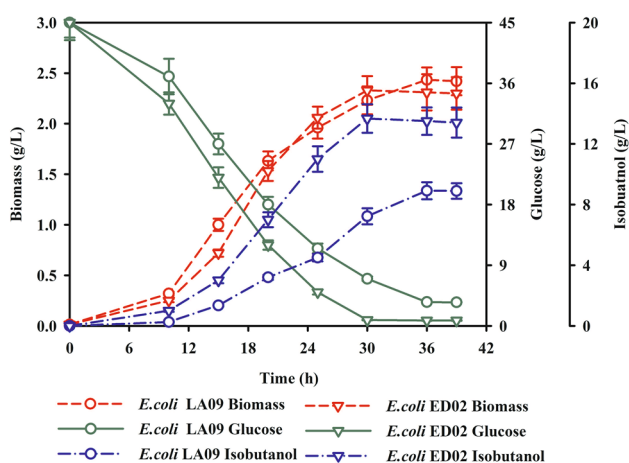
Fig. 6 The batch fermentation profiles of E. coli ED02 and E. coli LA09. The values shown represent the means of five independent experiments and the error bars represent standard deviations of five values

Therefore, one main goal of this work is to improve the glucose transformation into isobutanol.

As the rate of enzymatic reactions is regulated directly by the concentrations of substrates and products in cells, metabolomics is considered to be more closely connected to the physiology of organisms than the other "omics" approaches (i.e., transcriptomics and proteomics) [31, 38]. Therefore, the intracellular metabolic responses to different initial glucose concentration were deciphered during isobutanol fermentation. The results of multiple statistical analysis showed that the bypass flow seemed to be irrelevant to isobutanol synthesis, but the metabolites in glycolytic pathway, cofactor metabolism and stress response appeared to be closely connected with isobutanol production. It is not difficult to understand that cofactors (especially for redox cofactor) were limiting factors in isobutanol production, and most researchers attempted to improve redox status in isobutanol production [3, 34, 39]. Although the redox status had been modulated in our previous work [27], it was not optimal. Meanwhile, as the increase of initial glucose concentration, osmotic pressure of cells would be changed, which would induce the synthesis of some stress-related compounds, such as trehalose, L-glutamate and glutathione [18, 33, 45]. Notably, glycolytic pathway was the main pathway of the glucose transformation to isobutanol in strain *E. coli* LA09, the close connection between metabolites of glycolytic pathway and isobutanol production meant that glycolytic pathway may be a limiting factor in isobutanol production. The metabolomics analysis of the intermediate metabolites in glycolytic pathway showed that the upstream metabolites (G6P and F6P) were largely accumulated compared with the downstream metabolites as the increase of initial glucose concentration, which signified the reaction (F6P <-> FDP) from upstream metabolites to downstream metabolites may be a rate-limiting step.

It had been confirmed that only the single gene overexpression was very difficult to break the robustness of glycolytic pathway and increase the flux of glycolysis [13, 15, 16, 36, 41]. Here, we adopted a "bypass" method by reconstructing another pathway from glucose to isobutanol in strain *E. coli* LA09. On comparing the other three common carbon catabolism pathways (PP, PK and ED pathway) with glycolytic pathway, we chose ED pathway as the "bypass" to replace glycolytic pathway. The reasons were as follows: (1) ED pathway was more economical as the least reaction steps, which led to several-fold less protein cost than glycolytic pathway. Flamholz et al. [9] had convinced that although glycolytic pathway generated more ATP than ED pathway, organisms with a nonglycolytic source of ATP would tend to use ED pathway due to its lower protein cost. (2) More NADPH was generated by ED pathway, which was beneficial for the improvement of redox status in isobutanol production. (3) There was one

carbon loss per glucose by PP and PK pathway, respectively, but no carbon loss by ED pathway.

Preliminary tests showed the intracellular level of the toxic metabolite KDPG in *E. coli* ED01 harboring the whole ED pathway under the control of the strongest promoter BBa_J23119 was dramatically increased, which would be the major factor of cell growth inhibition [30]. The isobutanol titer and yield of *E. coli* ED01 were even lower than that of *E. coli* EDA only harboring the lower part of ED pathway. The main reason may be the inadaptive expression of ED pathway in host strain.

To solve the inadaptive expression of ED pathway, further modification of the upper part and lower part of ED pathway with various strength promoters was carried out. And the results suggested that the excess expression of the upper part of ED pathway would result in the accumulation of toxic KDPG, which would inhibit cell growth and own other negative effects in targeted products accumulation by stress depression [20], while the insufficient expression of the upper part of ED pathway would restrict the flux of ED pathway. Meanwhile, the high expression of the lower part of ED pathway would be benefit for glucose transformation and isobutanol production. The best isobutanol-producing strain *E. coli* ED02 was achieved with the moderate expression of upper part and high expression of lower part of ED pathway. The RT-PCR data also showed the two parts of ED pathway were tuned more reasonably. To the best of our knowledge, the enhancement of sugar utilization for rational improvement of isobutanol-producing *E. coli* was first reported by employing a redesigned heterologous artificial ED pathway in this work, while the improved and controllable of NADPH regeneration by the heterologous ED pathway had been designed [30].

In conclusion, to enhance sugar utilization for isobutanol production by strain development, metabolite reaction from F6P to FDP was identified as the rate-limiting step of glucose transformation to isobutanol by the intracellular metabolomics analysis. In view of the difficulty of breaking the glycolytic robustness, the ED pathway from *Zymomonas mobilis* was reengineered in isobutanol-producing *E. coli*. Finally, several engineered strains had been constructed using the various strength promoters, and the engineered strain *E. coli* ED02 showed the best fermentation properties. After 30 h fermentation of the strain *E. coli* ED02 with 45 g/L initial glucose, the isobutanol yield was increased by 47.4% to 0.50 C-mol/C-mol, reaching 74.6% of the maximal theoretical yield, and isobutanol titer was increased by 56.8% to 13.67 g/L compared with that of the start strain LA09, realizing the goal of enhancing sugar utilization for isobutanol production.

References

1. Atsumi S, Hanai T, Liao JC (2008) Non-fermentative pathways for synthesis of branched-chain higher alcohols as biofuels. Nature 451:86–U13. https://doi.org/10.1038/nature06450

2. Baez A, Cho K-M, Liao JC (2011) High-flux isobutanol production using engineered *Escherichia coli*: a bioreactor study with in situ product removal. Appl Microbiol Biotechnol 90:1681–1690. https://doi.org/10.1007/s00253-011-3173-y

3. Bastian S, Liu X, Meyerowitz JT, Snow CD, Chen MMY, Arnold FH (2011) Engineered ketol-acid reductoisomerase and alcohol dehydrogenase enable anaerobic 2-methylpropan-1-ol production at theoretical yield in *Escherichia coli*. Metab Eng 13:345–352. https://doi.org/10.1016/j.ymben.2011.02.004

4. Blombach B, Riester T, Wieschalka S, Ziert C, Youn J-W, Wendisch VF, Eikmanns BJ (2011) Corynebacterium glutamicum tailored for efficient isobutanol production. Appl Environ Microbiol 77:3300–3310. https://doi.org/10.1128/aem.02972-10

5. Buijs NA, Siewers V, Nielsen J (2013) Advanced biofuel production by the yeast *Saccharomyces cerevisiae*. Curr Opin Chem Biol 17:480–488. https://doi.org/10.1016/j.cbpa.2013.03.036

6. Chong L (2001) Molecular cloning—a laboratory manual, 3rd edition. Science 292:446. https://doi.org/10.1126/science.1060677

7. Conway T, Fliege R, Jones-Kilpatrick D, Liu J, Barnell WO, Egan SE (1991) Cloning, characterization and expression of the *Zymomonas mobilis* eda gene that encodes 2-keto-3-deoxy-6-phosphogluconate aldolase of the Entner–Doudoroff pathway. Mol Microbiol 5:2901–2911. https://doi.org/10.1111/j.1365-2958.1991.tb01850.x

8. Felpeto-Santero C, Rojas A, Tortajada M, Galan B, Ramon D, Garcia JL (2015) Engineering alternative isobutanol production platforms. AMB Express. https://doi.org/10.1186/s13568-015-0119-2

9. Flamholz A, Noor E, Bar-Even A, Liebermeister W, Milo R (2013) Glycolytic strategy as a tradeoff between energy yield and protein cost. Proc Natl Acad Sci USA 110:10039–10044. https://doi.org/10.1073/pnas.1215283110

10. Fu J, Wang Z, Chen T, Liu W, Shi T, Wang G, Y-j Tang, Zhao X (2014) NADH plays the vital role for chiral pure D-(-)-2,3-butanediol production in bacillus subtilis under limited oxygen conditions. Biotechnol Bioeng 111:2126–2131. https://doi.org/10.1002/bit.25265

11. Gaida SM, Liedtke A, Jentges AHW, Engels B, Jennewein S (2016) Metabolic engineering of *Clostridium cellulolyticum* for the production of *n*-butanol from crystalline cellulose. Microb Cell Fact. https://doi.org/10.1186/s12934-015-0406-2

12. Hao T, Han B, Ma H, Fu J, Wang H, Wang Z, Tang B, Chen T, Zhao X (2013) In silico metabolic engineering of *Bacillus subtilis* for improved production of riboflavin, Egl-237, (*R*, *R*)-2,3-butanediol and isobutanol. Mol BioSyst 9:2034–2044. https://doi.org/10.1039/c3mb25568a

13. Hauf J, Zimmermann FK, Muller S (2000) Simultaneous genomic overexpression of seven glycolytic enzymes in the yeast *Saccharomyces cerevisiae*. Enzym Microb Technol 26:688–698. https://doi.org/10.1016/s0141-0229(00)00160-5

14. Heckman KL, Pease LR (2007) Gene splicing and mutagenesis by PCR-driven overlap extension. Nat Protoc 2:924–932. https://doi.org/10.1038/nprot.2007.132

15. Huerta-Beristain G, Utrilla J, Hernandez-Chavez G, Bolivar F, Gosset G, Martinez A (2008) Specific ethanol production rate in ethanologenic *Escherichia coli* strain KO11 is limited by pyruvate decarboxylase. J Mol Microbiol Biotechnol 15:55–64. https://doi.org/10.1159/000111993

16. Jojima T, Inui M (2015) Engineering the glycolytic pathway: a potential approach for improvement of biocatalyst performance. Bioengineered 6:328–334. https://doi.org/10.1080/21655979.2015.1111493

17. Kalnenieks U (2006) Physiology of *Zymomonas mobilis* some unanswered questions. In: Poole RK (ed) Advances in microbial physiology, vol 51. Academic Press, Cambridge, pp 73–117. https://doi.org/10.1016/S0065-2911(06)51002-1

18. Kandror O, DeLeon A, Goldberg AL (2002) Trehalose synthesis is induced upon exposure of *Escherichia coli* to cold and is essential for viability at low temperatures. Proc Natl Acad Sci USA 99:9727–9732. https://doi.org/10.1073/pnas.142314099

19. Karabektas M, Hosoz M (2009) Performance and emission characteristics of a diesel engine using isobutanol-diesel fuel blends. Renew Energy 34:1554–1559. https://doi.org/10.1016/j.renene.2008.11.003

20. Kim J, Jeon CO, Park W (2008) Dual regulation of zwf-1 by both 2-keto-3-deoxy-6-phosphogluconate and oxidative stress in *Pseudomonas putida*. Microbiology SGM 154:3905–3916. https://doi.org/10.1099/mic.0.2008/020362-0

21. Kolodziej R, Scheib J (2012) Bio-isobutanol: the next-generation biofuel. Hydrocarb Processing 91:79+

22. Lara AR, Caspeta L, Gosset G, Bolivar F, Ramirez OT (2008) Utility of an *Escherichia coli* strain engineered in the substrate uptake system for improved culture performance at high glucose and cell concentrations: an fed-batch cultures. Biotechnol Bioeng 99:893–901. https://doi.org/10.1002/bit.21664

23. Li S, Huang D, Li Y, Wen J, Jia X (2012) Rational improvement of the engineered isobutanol-producing *Bacillus subtilis* by elementary mode analysis. Microb Cell Fact. https://doi.org/10.1186/1475-2859-11-101

24. Li S, Wen J, Jia X (2011) Engineering *Bacillus subtilis* for isobutanol production by heterologous Ehrlich pathway construction and the biosynthetic 2-ketoisovalerate precursor pathway overexpression. Appl Microbiol Biotechnol 91:577–589. https://doi.org/10.1007/s00253-011-3280-9

25. Li S, Xu N, Liu L, Chen J (2014) Engineering of carboligase activity reaction in *Candida glabrata* for acetoin production. Metab Eng 22:32–39. https://doi.org/10.1016/j.ymben.2013.12.005

26. Lin Z, Xu Z, Li Y, Wang Z, Chen T, Zhao X (2014) Metabolic engineering of *Escherichia coli* for the production of riboflavin. Microb Cell Fact. https://doi.org/10.1186/s12934-014-0104-5

27. Liu J, Qi H, Wang C, Wen J (2015) Model-driven intracellular redox status modulation for increasing isobutanol production in *Escherichia coli*. Biotechnol Biofuels. https://doi.org/10.1186/s13068-015-0291-2

28. Liu Y, Zhou H, Wang L, Wang S, Fan L (2016) Improving *Saccharomyces cerevisiae* growth against lignocellulose-derived inhibitors as well as maximizing ethanol production by a combination proposal of gamma-irradiation pretreatment with in situ detoxification. Chem Eng J 287:302–312. https://doi.org/10.1016/j.cej.2015.10.086

29. Lu J, Brigham CJ, Gai CS, Sinskey AJ (2012) Studies on the production of branched-chain alcohols in engineered *Ralstonia eutropha*. Appl Microbiol Biotechnol 96:283–297. https://doi.org/10.1007/s00253-012-4320-9

30. Ng CY, Farasat I, Maranas CD, Salis HM (2015) Rational design of a synthetic Entner–Doudoroff pathway for improved and controllable NADPH regeneration. Metab Eng 29:86–96. https://doi.org/10.1016/j.ymben.2015.03.001

31. Nie L, Wu G, Culley DE, Scholten JCM, Zhang W (2007) Integrative analysis of transcriptomic and proteomic data: challenges, solutions and applications. Crit Rev Biotechnol 27:63–75. https://doi.org/10.1080/07388550701334212

32. Perrenoud A, Sauer U (2005) Impact of global transcriptional regulation by ArcA, ArcB, Cra, Crp, Cya, Fnr, and Mlc on glucose catabolism in *Escherichia coli*. J Bacteriol 187:3171–3179. https://doi.org/10.1128/jb.187.9.3171-3179.2005

33. Purvis JE, Yomano LP, Ingram LO (2005) Enhanced trehalose production improves growth of *Escherichia coli* under osmotic stress. Appl Environ Microbiol 71:3761–3769. https://doi.org/10.1128/aem.71.7.3761-3769.2005

34. Qi H, Li S, Zhao S, Huang D, Xia M, Wen J (2014) Model-driven redox pathway manipulation for improved isobutanol production in *Bacillus subtilis* complemented with experimental validation and metabolic profiling analysis. PLoS One. https://doi.org/10.1371/journal.pone.0093815

35. Rogers PL, Jeon YJ, Lee KJ, Lawford HG (2007) *Zymomonas mobilis* for fuel ethanol and higher value products. In: Olsson L (ed) Biofuels, vol 108. Advances in biochemical engineering-biotechnology. Springer, Berlin, Heidelberg, pp 263–288. https://doi.org/10.1007/10_2007_060

36. Schaaff I, Heinisch J, Zimmermann FK (1989) Overproduction of glycolytic enzymes in yeast. Yeast (Chichester, Engl) 5:285–290. https://doi.org/10.1002/yea.320050408

37. Schmittgen TD, Livak KJ (2008) Analyzing real-time PCR data by the comparative C-T method. Nat Protoc 3:1101–1108. https://doi.org/10.1038/nprot.2008.73

38. Schuetz R, Zamboni N, Zampieri M, Heinemann M, Sauer U (2012) Multidimensional optimality of microbial metabolism. Science 336:601–604. https://doi.org/10.1126/science.1216882

39. Shi A, Zhu X, Lu J, Zhang X, Ma Y (2013) Activating transhydrogenase and NAD kinase in combination for improving isobutanol production. Metab Eng 16:1–10. https://doi.org/10.1016/j.ymben.2012.11.008

40. Smith KM, Cho K-M, Liao JC (2010) Engineering *Corynebacterium glutamicum* for isobutanol production. Appl Microbiol Biotechnol 87:1045–1055. https://doi.org/10.1007/s00253-010-2522-6

41. Snoep JL, Yomano LP, Westerhoff HV, Ingram LO (1995) Protein burden in *Zymomonas mobilis*: negative flux and growth control due to overproduction of glycolytic enzymes. Microbiology 141:2329–2337

42. Wang B-W, Shi A-Q, Tu R, Zhang X-L, Wang Q-H, Bai F-W (2012) Branched-chain higher alcohols. In: Bai FW, Liu CG, Huang H, Tsao GT (eds) Biotechnology in China III: biofuels and bioenergy, vol 128. Advances in biochemical engineering-biotechnology. Springer, Berlin, Heidelberg, pp 101–118. https://doi.org/10.1007/10_2011_121

43. Wang C, Liu J, Liu H, Liang S, Wen J (2017) Combining metabolomics and network analysis to improve tacrolimus production in *Streptomyces tsukubaensis* using different exogenous feedings. J Ind Microbiol Biotechnol 44:1527–1540. https://doi.org/10.1007/s10295-017-1974-4

44. Xia M, Huang D, Li S, Wen J, Jia X, Chen Y (2013) Enhanced FK506 production in *Streptomyces tsukubaensis* by rational feeding strategies based on comparative metabolic profiling analysis. Biotechnol Bioeng 110:2717–2730. https://doi.org/10.1002/bit.24941

45. Zhang J, Fu R-Y, Hugenholtz J, Li Y, Chen J (2007) Glutathione protects *Lactococcus lactis* against acid stress. Appl Environ Microbiol 73:5268–5275. https://doi.org/10.1128/aem.02787-06